THE PENNSYLVANIA STATE UNIVERSITY
SCHREYER HONORS COLLEGE

DEPARTMENT OF CHEMISTRY

DEVELOPMENT OF CATALYSTS FOR THE HYDROGEN EVOLUTION REACTION AND AMMONIA BORANE HYDROLYSIS

TAYLOR SOUCY
SPRING 2017

A thesis
submitted in partial fulfillment
of the requirements
for a baccalaureate degree
in Chemistry
with honors in Chemistry

Reviewed and approved* by the following:

Raymond Schaak
Professor of Chemistry
Thesis Supervisor

Raymond Funk
Professor of Chemistry
Honors Adviser

Katherine Masters
Senior Lecturer of Chemistry
Committee Reader

* Signatures are on file in the Schreyer Honors College.

ABSTRACT

Global energy demands are expected to be 27 TW by 2040, up from the current level of 13 TW. Meeting this requirement by current methods of fuel production, the burning of fossil fuels, results in the production of harmful sulfur, carbon, and nitrogen-based pollutants. Photoelectrochemical cells are a promising alternative energy platform, producing clean-burning hydrogen fuel from water with oxygen as the only byproduct. In this device, hydrogen is produced at the cathode (hydrogen evolution reaction, HER) and oxygen is produced at the anode (oxygen evolution reaction, OER). For this technology to be industrially viable, earth abundant and inexpensive HER and OER catalysts need to be discovered. Additionally, a method for the storage and transportation of hydrogen as a solid must be developed to minimize shipping costs. Here, we show that molybdenum rich Co-Mo nanoparticles are effective catalysts for the HER. We also describe recent discoveries in our lab towards the implementation of promising catalysts for the hydrolysis of a hydrogen storage material, ammonia borane.

TABLE OF CONTENTS

LIST OF FIGURES

LIST OF TABLES

ACKNOWLEDGEMENTS

I'd like to thank Dr. Ray Schaak, the exceptional scientist and adviser who allowed me to work in his research group for 3 years. His brilliant support, advice, and mentorship from the very beginning of my research career as a freshman has made me into the scientist that I am today. I am so thankful that I was able to be a part of a group that is so helpful, smart and kind. I'd like to thank each member of this lab who had a positive impact on me as a scientist, especially Julie Fenton, who took time to give me advice and mentorship when researching became extremely difficult. I'd also like to thank my committee readers, the brilliant Dr. Ray Funk and Dr. Kate Masters, for taking the time to critique my thesis and my defense. Dr. Funk and Dr. Masters have also been great advisers throughout my time here at Penn State and have each given me the chance to TA and grow a heart for teaching; I'm extremely grateful for the time that they have taken to guide me toward my goals and overcome substantial challenges towards the completion of this thesis and my undergraduate degree.

I am thankful to Dr. Eric Popczun, my first mentor, for teaching me all about research and nanoparticles. I became a passionate researcher because of his excitement for science. I am also thankful for Dr. Josh McEnaney, who helped me through my first successful project and motivated me to work hard and learn more in lab. Finally, I'd like to thank my amazing mentee, Catherine Badding. The ammonia borane project would not have been as successful without the time that she put in.

Chapter 2 was funded by the National Science Foundation (NSF) Center for Chemical Innovation in Solar Fuels (CHE-1305124). TEM, HRTEM, STEM-EDS, and XPS data were acquired at the Materials Characterization Laboratory of the Penn State Materials Research

Institute. In addition to the co-authors on the paper, I'd like to thank Carlos Read, Greg Barber, and Vincent Bojan for technical support and helpful discussions.

To my wonderful family: thank you. Both my immediate and Millennium families had a huge part in getting me to where I am today. I am endlessly thankful for Star Sharp, Dr. Nate Brown, and Dean Mary Beth Williams who supported me throughout my undergraduate career, especially at the beginning when I doubted myself. MSP cohorts 1, 2 and 3 have been a huge source of support for me, and I am incredibly grateful for their friendship and love through the hard times. To all of my friends who drank coffee with me and had countless study sessions in the Wolf study rooms or in the Atherton lobby, I am thankful for you. Each of my college roommates (Emma, Victoria, Becca, and Alice) were such strong pillars of support in my life and I am thankful for each of them; my "brother"/running bud, Dan, and my cousins Gabby and Olivia were wonderful additions to and kept me sane at Penn State. I couldn't have made it without the support of my home friends and family, including Becca, Sage, and Morgan. The most important people in my life are my parents; my little siblings, Anthony and Elizabeth; and my wonderful best friend of nearly four years, Nico (and his amazing family). To my mom, dad, Ant, El, and Nico: I wouldn't have made it without you. I am endlessly grateful for your support.

Most importantly, I am thankful that my Heavenly Father put me on this earth and gave me the courage to pursue a career of chemistry. Thank You for giving me the strength when I think it's too hard, for giving me a heart of curiosity for research, and for showing me Your beauty each day in Your world. The world of chemistry and science is truly a proof of His existence and I thank Him for giving me eyes to see that each and every day that I read and learn and research

Chapter 1: Introduction

The burning of wood, coal, oil, and natural gas has powered the human population throughout history.[1] The use of these nonrenewable energy sources powered the Industrial Revolution, catapulting the economy and technology sectors since the 18th century.[2]

The energy needs of the global economy are increasing, with global power use projected to grow from 17 TW in 2010 to 27 TW by 2040.[3] The exponential energy use increase has largely been facilitated by nonrenewable energy sources – coal, petroleum, and natural gas, as seen in Fig. 1.[4]

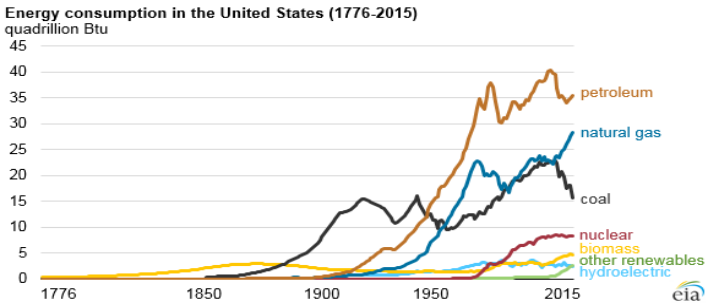

Figure 1: While renewable energy sources are growing in use, the burning of fossil fuels still dominate the energy market.

The major problem with the combustion of fossil fuels is not the supply – although it is finite, global supply of these energy sources to last society at least several generations.[2] The production of carbon dioxide upon combustion of these fuels is the larger issue, as the atmospheric concentration of CO_2 has reached unprecedented levels, as seen in Fig. 8.[5]

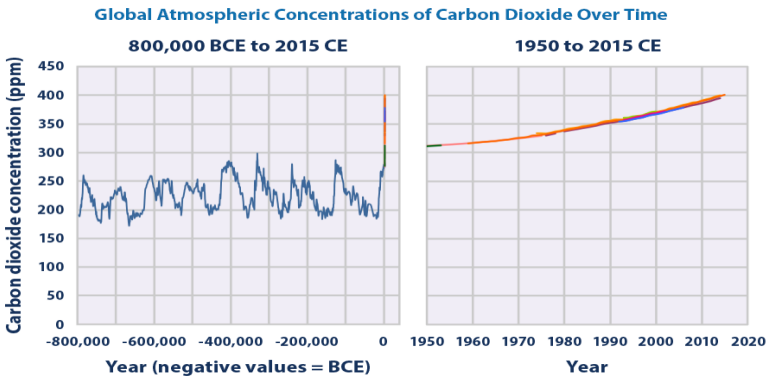

Figure 2: The atmospheric concentration of carbon dioxide has reached levels higher than at any point in recent history.[5]

The carbon dioxide produced over the next 40 years will persist for the next 500-2,000 years due to its equilibration between the atmosphere and the oceans every 30-40 years and the lack of a natural destruction mechanism.[6] While the shift from burning of wood to coal to oil to natural gas has led to a decrease in the mean intensity of CO_2 production per year (due to the increase in the H:C, respectively) the global population increase will likely result in increased global carbon emission accumulation.[6] The increase in atmospheric carbon dioxide concentrations have created an enhanced greenhouse effect, leading to an increase in global temperatures.[7] A major societal goal has been to keep the average temperature to less than 2˚C above the temperature from the preindustrial era, which might limit potentially catastrophic environmental effects. Many models have predicted that in order to have a greater than 50% chance to achieve this target, large scale-deployment of negative emissions technologies must take place and the reduction in production of carbon dioxide via alternative energy technologies must be realized.[8] The implementation of a hydrogen economy may be a feasible option to enable a clean energy future.[9]

Hydrogen is widely regarded to be a clean fuel that may replace natural gas and oil as a future energy source.[10] Hydrogen is an excellent energy carrier because it is very stable and environmentally friendly when used for energy in a fuel cell.[11] When combined with oxygen in a fuel cell, a reaction is catalyzed that produces energy with a $\Delta H°$ of -242 kJ/mol, and a $\Delta G°$ of -229 kJ/mol (**Reaction 1**).[12] Because of their capability to produce large amounts of energy and lack of harmful byproducts, fuel cells are a promising alternative energy platform.

$$H_2(g) + ½\ O_2(g) \rightarrow H_2O(l)\ \Delta H° = -242\ kJ/mol\ \Delta G°=-229\ kJ/mol$$ **Reaction 1**

Figure 1 shows an example of a fuel cell, which functions by combining gaseous hydrogen and oxygen from two different channels to generate electricity. Hydrogen interacts with a material that catalyzes the decomposition of hydrogen to 2 H^+ ions and 2 electrons.[12] The protons travel across an ion-exchange membrane to another catalyst, where they react with O_2 and electrons to form water. The flow of electrons between the two catalysts creates a current that can be used to power devices. No harmful gases, such as CO or CO_2, nitrogen oxides (NO_x) or sulfur oxides (SO_x) gases, are produced.[13]

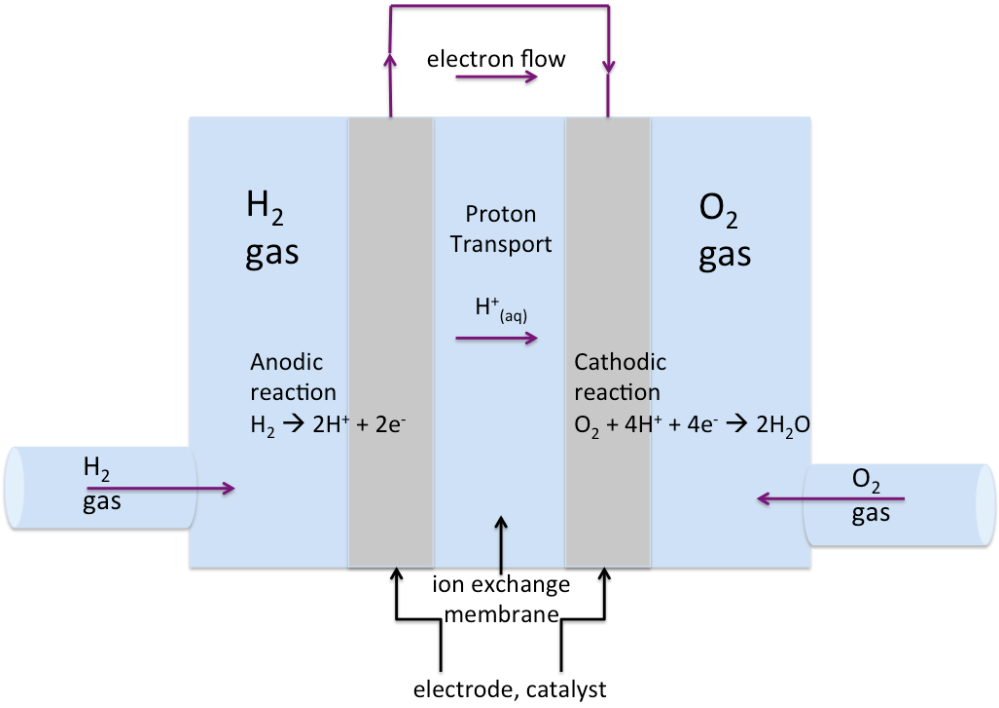

Figure 3: A fuel cell catalyzes the combination of hydrogen and oxygen gas to energy and water.

For fuel cell technology to be commercially relevant, hydrogen must be produced cheaply and efficiently in large quantities. Currently, the production of hydrogen is accomplished by the steam methane reformation of fossil fuels, which results in the formation of greenhouse gases.[14] Petroleum, diesel, and propane steam reformation are used to produce H_2 and CO (**Reaction 2**) with temperatures in excess of 700°C.[15,16]

$$CH_4\,(g) + H_2O(g) + \text{heat} \rightarrow CO(g) + 3H_2(g) \quad \textbf{Reaction 2}$$

The CO can be captured and reacted with a catalyst and more steam to produce more hydrogen (**Reaction 3**).[17]

$$CO(g) + H_2O(g) \rightarrow H_2(g) + CO_2(g) + \text{heat} \quad \textbf{Reaction 3}$$

For the entire reaction scheme above, $\Delta H°_{298K} = 165.2$ kJ/mol, making it energetically unfavorable.

Photoelectrochemical cells (PECs) that perform water splitting are an example of a solar to hydrogen (STH) strategy, solving the problem of large energy inputs and hydrocarbon use to generate hydrogen gas. Dubbed artificial photosynthesis due to its mechanistic similarity to the process used by nature to store energy from the sun in chemical bonds, PECs work by using sunlight and catalysts to convert water into hydrogen and oxygen (**Reaction 4**).[18] This process is advantageous over other STH systems because of its simplicity and lack of harmful byproducts, and is therefore a promising clean energy platform.[15] The overall reaction is endothermic, but the use of solar energy can overcome the energy barrier without the production of harmful greenhouse gases. The use of catalysts reduces the energy barrier required to overcome the water splitting reaction.

$$2H_2O(l) \rightarrow 2H_2(g) + O_2(g) \qquad \Delta G°=237\text{kJ/mol} \qquad \textbf{Reaction 4}$$

The use of catalysts to produce hydrogen using the hydrogen evolution reaction (HER) will be discussed in Chapter 2.

If hydrogen is to be produced by STH (PEC or otherwise), a further problem manifests itself in the transportation of the gas. There are no pipelines or networks to transport hydrogen like there are for natural gas or oil.[10] Therefore, new transportation infrastructure to needs to be developed. Additionally, the US Department of Energy mandated that hydrogen fuel cell electric vehicles (FCEV) are required to exhibit a driving range of 300 miles without adding a large amount of weight or volume to the vehicle.[19] This is an issue, because the 5 kilograms of hydrogen needed to power a vehicle for 300 miles occupies a volume of 54 m^3 (at standard temperature and pressure).[20] This volume does not meet DOE targets for hydrogen mass or weight density and is not feasible for large-scale transportation. Two strategies to circumvent this volume problem are to compress or liquefy hydrogen (decrease its volume) or store it chemically using a molecule so that it can be released when needed.[20] Additional energy inputs are also required to compress or liquefy hydrogen. The chemical storage of hydrogen is a useful alternative.

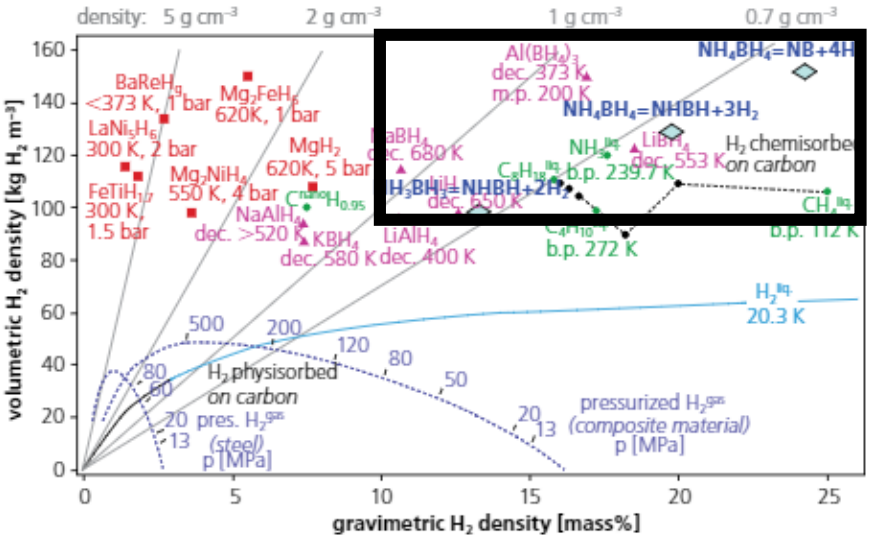

Figure 4: Plot of volumetric vs. gravimetric density of diatomic hydrogen with potential hydrogen storage materials plotted. The DOE target for 2015 is the black bolded box. [10]

Among other solutions, ammonia borane has been put forth as a promising candidate for a hydrogen storage material.[21] This molecule is a highly polar, which explains its high melting temperature in comparison to its isoelectronic counterpart, ethane. AB is nontoxic, soluble in water, and produces 3 molar equivalents of hydrogen when treated with a catalyst.[22] The most effective catalyst for this reaction is platinum, but the implementation of this system on a global scale would require catalysts that are earth abundant and inexpensive.[23,24] The discovery of catalysts for the hydrolysis of ammonia borane is discussed in Chapter 3.

Chapter 2: Catalyst for the Hydrogen Evolution Reaction

The work in this chapter was done in collaboration with Dr. Joshua McEnaney, Dr. Juan Callejas, Dr. James Hodges, and Jared Mondschein and was published in the Royal Society of Chemistry's Journal of Materials Chemistry A.[25] My contributions included the initial synthesis, characterization, and electrochemical testing of the Co-Mo nanoparticles.

2.1 Introduction

With carbon dioxide levels rising to record levels, taking advantage of freely available sunlight to create hydrogen for fuel applications is of paramount importance.[26] Photoelectrochemical (PEC) water splitting uses solar energy to split water into hydrogen and oxygen by the corresponding hydrogen or oxygen evolution reactions, which take place at the cathode and anode, respectively.[18] A major issue that impedes the progress of sunlight-driven renewable energy is the search for catalysts.[27] While nature had devised organic molecules that assist in the conversion from solar energy to chemical energy, scientists have yet to develop catalysts that are sustainably derived, stable, and inexpensive. [27]

To date, the most effective hydrogen evolution catalyst is Pt, showing the lowest overpotentials measured at the standard benchmarking current density of -10 mA cm^{-2}.[28] However, mass implementation of Pt as a catalyst is not practical due to its limited Earth-abundance, preventing wide-scale implementation.[29] A PEC requires electrolytic conditions, and usually employs highly acidic or highly alkaline conditions.[28] It is useful for PECs to have both the oxygen evolution reaction and the hydrogen evolution reaction take place in the same pH conditions. While many

OER catalysts are active and stable in alkaline aqueous solutions, HER catalysts still need to be developed for use in these conditions.[30] While there have been advances in the HER catalysts in acidic aqueous solution over the last ten years, including classes of sulfides, carbides, and phosphides, more work must be done in order to achieve low overpotentials for the HER in alkaline solutions.[31]

Molybdenum-containing compounds have been studied for the HER in acidic systems (MoS_2,[32] Mo_2C,[33] and MoB,[33] and MoP,[34] were all highly active in acidic media). 3d transition metal alloys such as Ni-Mo and Co-Mo are highly active and stable electrocatalysts in alkaline solutions.[35,36] These alloys have been synthesized via electrodeposition, which results in a low surface areas, but catalytic effectivity may be improved by further increasing the surface area of the catalyst.[37] The goal of this work was to synthesize Co-Mo alloy nanoparticles using colloidal methods and test the electrocatalytic properties of the material for the HER.

2.2 Experimental

Materials and chemicals:

The following materials were used as purchased without further purification: squalane [98%, $C_{30}H_{62}$, Alfa-Aesar], oleylamine [70%, C18H27N, Sigma-Aldrich], molybdenum hexacarbonyl [98%, $Mo(CO)_6$, Sigma-Aldrich], dicobalt octacarbonyl [>90% (Co), 1-10% hexanes, $Co_2(CO)_8$, Sigma-Aldrich], and sulfuric acid [99.999%, Sigma-Aldrich]. The following items were used for electrode preparation and testing: titanium foil [99.7%, 0.25 mm thickness, Sigma Aldrich], Ag paint [high quality, SPI supplies, and two-part epoxy [HYSOL 9460, Henkel Corp].

Synthesis of Cobalt-Molybdenum nanoparticles:

NPs were synthesized in a 50 mL three-necked round-bottom flask equipped with reflux condenser, thermometer adapter, rubber septum, and stirbar. 7.0 mL of squalene and 0.2 mL oleylamine were added to the round-bottom flask and degassed for 20 minutes at 120˚C while continuously stirred. The mixture was cooled to 50˚C after being placed under a blanket of argon gas. 132 mg of $Mo(CO)_6$ was added to the solution, and the mixture was heated to 120˚C. In a separate Ar-filled septum capped vial, 100 mg of $Co_2(CO)_8$ was dissolved in 0.5 mL of hexanes and 2 mL of squalene. The $Co_2(CO)_8$ solution was injected into the round bottom flask at 120˚C; the resulting mixture was heated to 320˚C and remained at this temperature for 20 minutes. The solution was allowed to cool to room temperature. The reaction mixture was transferred to a centrifuge tube. Volumes of 7.5 mL hexanes and 15 mL ethanol were added to the centrifuge tube. The mixture was then centrifuged at 12,000 rpm for 3 minutes. The resulting pellet was redispersed in hexanes, and the washing process was repeated by adding 2:1 ratio of hexanes to ethanol before characterization.

Preparation of working electrodes:

Electrodes for electrochemical characterization were prepared as previously described.[29,34,38] Titanium foil was cut into 0.2 cm^2 substrates. The Co-Mo nanoparticles, dispersed in hexanes, were drop-cast onto the foils in 5µL increments to achieve a loading of approx. 1 mg cm^{-2}. After drying, Co-Mo/Ti foils were heated in a tube furnace at 350˚C under H_2(5%)/Ar(95%) to remove surfactant molecules. The foils were then attached to polyvinyl chloride-coated Cu wire using Ag

paint. To ensure that the surfaces were insulated, two-part epoxy was applied and allowed to dry before electrochemical characterization. The final particle loading density was determined by the use of a microbalance and a high-resolution scanner to determine electrode surface area.

Electrochemical characterization:

Electrochemical measurements were performed using a Gamry Instruments Reference 600 potentiostat. All measurements were performed in 1.0 M KOH in a standard three-electrode cell. The cell contained a graphite counter electrode and a Hg/HgO reference electrode. All polarization data were acquired with a sweep rate of 2 mV s^{-1} while research grade H_2(g) was continuously bubbled through the electrolyte solution under rapid stirring. The reversible hydrogen electrode (RHE) potential was determined by measuring the open-circuit potential of a clean Pt electrode in the electrolyte solution after testing the non-noble metal electrodes. Initial stability tests were performed galvanostatically by holding at an applied current density of -10 mA cm^{-2} for 18 h. Long-term tests for electrochemical stability were acquired using voltammetric sweeps, cycling 500 times between +0.15 and -0.15 V vs. RHE at 100 mV s^{-1}. After electrochemical testing, measurement of the open-circuit potential of a clean Pt mesh electrode allowed for the determination of the RHE potential in the electrolyte solution. Quantitative hydrogen yield measurements were performed by passing a cathodic current of 10mA continuously through the 0.2 cm^2 working electrode for 50 min (3000 s for 30 C of charge). Hydrogen bubbles evolved from the working electrode were captured in an inverted graduated cylinder containing the 1 M KOH electrolyte.

Materials characterization:

The Co-Mo nanoparticles were dispersed in a hexane solution and drop-cast (0.7μL) onto a 400 mesh Formvar and carbon-coated Cu grid (Electron Microscopy Sciences) for characterization by transmission electron microscopy (TEM). TEM images were obtained using a JEOL 1200 microscope with accelerating voltages of 80 kV. Powder X-ray diffraction (XRD) patterns were acquired using a Bruker-AXS D8 Advance diffractometer with CuKα radiation and a LynxEye 1-D detector. Simulated XRD patterns were generated using the CrystalMaker/CrystalDiffract software package. High-angle annular dark-field scanning transmission electron microscopy (HAADF-STEM) images were collected using an FEI Titan G2 S/TEM at an accelerating voltage of 200 kV. Energy dispersive X-ray spectroscopy (EDS) maps were also acquired with an FEI Titan, using the Super-X EDX quad detector system at a current of ~0.15 nA. Standardless Cliff-Lorimer quantification was performed on the deconvoluted EDS line intensity data using the Bruker Esprit software. Brunauer-Emmert-Teller (BET) surface area measurements using a Quantachrome Autosorb iQ3 at liquid nitrogen temperatures, and the data were analyzed using ASiQwin software version 3.01 (2013). X-ray photoelectron spectroscopy (XPS) was acquired using Al(Kα) radiation (1486 eV) in a PHI VersaProbe Scanning XPS microphobe.

2.3 Results and Discussion

Characterization of nanoparticles:

The thermal decomposition of $Mo(CO)_6$ and $Co(CO)_8$ resulted in the synthesis of the Co-Mo nanoparticles. The decomposition took place in the presence of oleylamine and squalane at

320˚C. The product is shown in Fig. 1a, a TEM image of the nanoparticles. The average diameter of the nanoparticles is 3 ± 1 nm. The sample is not crystalline, as evidenced by the broad scattered electron diffraction (SAED) pattern (Fig. 1b) and the lack of peaks in the powder XRD pattern (Fig. 1c).

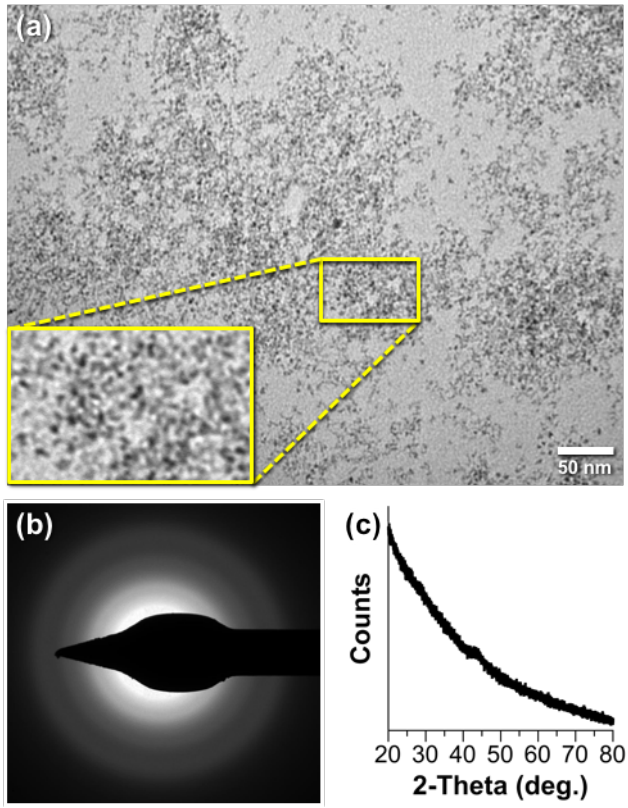

Figure 5: (a) TEM image showing the synthesized nanoparticles and the corresponding (b) SAED pattern and (c) XRD pattern. Reproduced from Ref. 1 with permission from the Royal Society of Chemistry.[25]

The identity of the particles was confirmed via STEM imaging. These figures show that the particles have a 3 nm particle diameter (Fig. 2a), as well as the short-range

crystalline order. This data, in combination with the XRD and SAED patterns, confirms the existence of a weakly crystalline material.

STEM-EDS mapping showed that the atomic ratio of Co:Mo in the nanoparticles was 1:9. The Co, Mo, and Co + Mo element maps were collected from EDS data (Fig. 4b-d). The mapping shows that both the Co and Mo elements are dispersed throughout the nanoparticles.

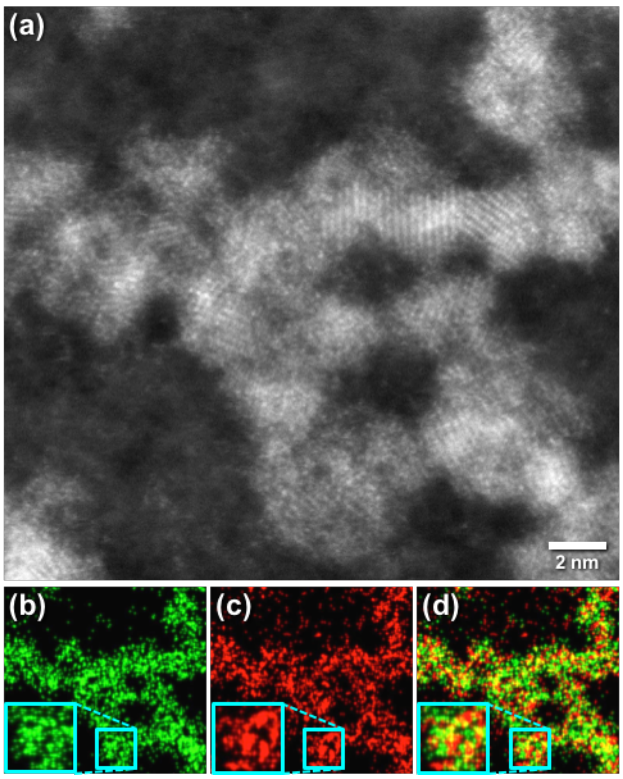

Figure 6(a) HAADF-STEM image of the synthesized Co-Mo nanoparticles and corresponding STEM-EDS element maps for (b) Co, (c) Mo, and (d) Co + Mo. Reproduced from Ref. 2 with permission from the Royal Society of Chemistry.[25]

Electrochemical data:

In order to test the electrocatalytic activity of the Co-Mo nanoparticles, the particles (suspended in hexanes) were loaded onto Ti foils with a density of 1 mg cm^{-2}. The Ti substrates were prepared for electrochemical testing by annealing for 2 h at 350˚C in H_2(5%)/Ar(95%). This annealing process resulted in the elimination of ligands that surrounded the nanoparticles due to the colloidal synthesis method. The nanoparticles were tested in strongly alkaline conditions (1M KOH). Fig. 5 shows the activity of the Co-Mo nanoparticles against a bare, inactive Ti foil and, for comparison, the highly active Pt mesh.

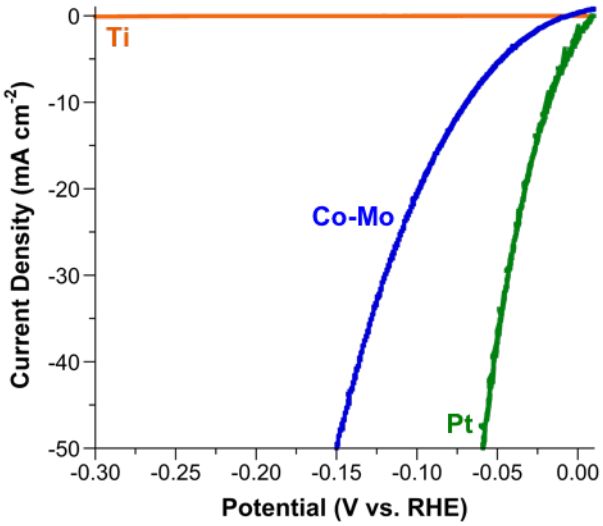

Figure 7: Electrochemical data for the synthesized Co-Mo nanoparticles, the highly active Pt benchmark, and the bare and inactive Ti foil. Reproduced from Ref. 3 with permission from the Royal Society of Chemistry.[25]

At the commercially relevant current density of - 10 mA cm^{-1}, the synthesized Co-Mo nanoparticles required an overpotential of only -75 mV. For comparison, the highly active benchmark Pt produces -10 mA cm^{-1} with an overpotential of -25 mV in 1 M KOH. The Co-Mo

catalysts presented here perform much better than previous studies that utilized Co-Mo as catalysts for the hydrogen evolution reaction – these studies report overpotentials of up to -100 mV are required to achieve -10 mA cm^{-2}.[30] The lower overpotential shown herein is likely due to the high surface area of the Co-Mo nanoparticles. Additionally, the data presented here rivals the extensively studied Ni-Mo compound, which produces hydrogen at an overpotential of -30 to -130 mV at -10 mA cm^{-2}.

The stability of the nanostructured Co-Mo electrocatalyst for the HER at pH 14 was tested by cyclic voltammetry. No significant changes in performance was observed after 500 cycles between +0.15 and -0.15 V vs. RHE (Fig. 6a). Further stability tests were performed by subjecting the Co-Mo/Ti electrodes galvanostic experiments at a constant current density of -10 mA cm^{-2} for 18 h (Fig. 6b). With no significant change in overpotential over this time period, the nanoparticles were determined to be stable catalysts in highly alkaline conditions for the hydrogen evolution reaction.

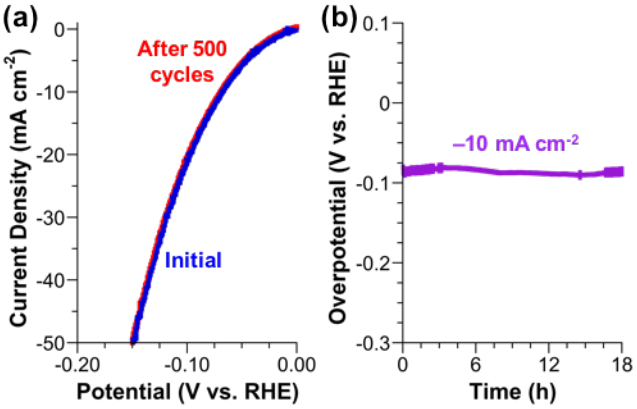

Figure 8. (a) 500 cyclic voltammograms in 1 M KOH and (b) galvanostic results after 18 h, showing no change in overpotential. Reproduced from Ref. 4 with permission from the Royal Society of Chemistry.[25]

2.4 Conclusions

A new synthesis was designed to produce molybdenum rich Co-Mo nanoparticles, which are excellent catalysts for the hydrogen evolution reaction. The nanoparticles contain clusters of 1 nm crystalline domains and both elements are homogeneously dispersed throughout. The electrochemical activity confirmed that the Co-Mo nanoparticles were highly active for the hydrogen evolution reaction, requiring an overpotential of just -75 mV at the industrially relevant current density of -10 mA cm^{-2}. Additionally, the nanoparticles were determined to be stable in alkaline media by cyclic voltammetry and galvanostatic experiments.

Chapter 3: Catalysts for Ammonia Borane Hydrolysis

The work in this chapter was done in collaboration with Catherine Badding, who handled the synthesis and screening of bulk powders and assisted with catalytic experiments.

Chapter 3.1 Introduction

As discussed in Chapter 1, ammonia borane is a viable hydrogen storage option, which will be important for a chemical hydrogen storage method should a hydrogen economy become implemented on a large scale.

The chemical storage of hydrogen remains a much more feasible strategy than a pressurized or cooled system. In this way, hydrogen is stored in a molecule, only to be released when the decomposition of that molecule occurs. An ideal molecule would have a high hydrogen content by weight, possess a low heat of dehydrogenation in order to use a minimum amount of energy to release the hydrogen, and have high rates of reaction between 80-120°C (the operating temperatures of a fuel cell).[39] The DOE's goals for 2015 are to have a molecule with at least 9 wt% H_2, a volumetric density of greater than 82 (kg H_2) m^{-3} and a transportation temperature between -20 °C and 85 °C.[40]

Ammonia borane ($H_3B—NH_3$, AB) is a good candidate for such a system. First synthesized in 1955,[41] it is isoelectronic with ethane (a gas at room temperature), but is highly polar and therefore has a boiling point 284°C, higher than that of ethane.[20] Its melting point is 112°C,

making it a stable solid at room temperature and therefore denser than hydrogen gas.[42] AB has a molecular weight of 30.7 g/mol, is 19.6 wt% H_2, and has a density of 145 $kg_{H2}\,m^{-3}$.[42] It meets the storage, transportation, and wt% parameters set by the DOE.[40] AB is also soluble and stable in water (and other polar solvents) and is nontoxic, all necessary requirements for achieving commercial relevance.[43]

Ammonia borane has the potential to release 3 equivalents of H_2 by the following reaction:[44]

$$NH_3BH_3(aq) + 2H_2O(l) \rightarrow NH_4^+(aq) + BO_2^-(aq) + 3H_2(g) \quad \textbf{Reaction 5}$$

This reaction involves the dissolution of ammonia borane in a protic solvent (alcohols such as methanol would also be sufficient).[21] Unlike other hydride storage system, AB doesn't require harsh basic conditions to release hydrogen for its decomposition.[45] The thermal decomposition of AB occurs at three different temperatures: 120, 150, and 500 °C. These can be measured by pressure increases while heating the system.[20]

$$nNH_3BH_3 \rightarrow (NH_2BH_2)_n + (n-1)H_2 \quad <120\ °C$$

$$(NH_2BH_2)_n \rightarrow (NHBH)_n + H_2 \quad ----150\ °C$$

$$2(NHBH)_n \rightarrow (NHB—NBH)_n + H_2 \quad --- 150\ °C$$

$$(NHBH)_n \rightarrow BN + H_2 \quad >500\ °C$$

Each temperature setpoint releases 6.5 wt% H_2, but because undesirable byproducts are produced above 150 °C (ammonia, diborane, and borazine), only 13 wt% is captured using thermal decomposition.[43] Borazine, for example, is undesirable because it will poison the fuel cells.[46] For this reason, other methods to liberate hydrogen from AB are of great scientific interest. Three such techniques to release hydrogen from ammonia borane are transition metal-catalyzed dehydrogenation, ionic liquid-catalyzed dehydrogenation, and nanophase ammonia borane encapsulated in SBA-15.[20]

Ionic liquids are salts that are liquids below 100°C. Their properties include low vapor pressure, high stability at increased temperatures, high dissolution ability, and facile recycling.[47] Though these catalysts have some advantageous properties, the catalytic decomposition using ionic liquids did not produce the optimal 3 equiv of H_2. For example, Bluhm et al. only produced a maximum of 1.5 equiv over several hours,[47] while Himmelberger et al produced 2.2 equiv H_2 and took 20 minutes.[48] This still meets the DOE's standard of 9 wt% H_2.

Nanoscale transition metal catalysts have been shown to serve as favorable catalysts for AB hydrolysis.[44] A wide variety of different transition metal catalysts have been tested, including Fe nanoparticles,[49] Ni nanoparticles,[50] and several noble metal catalysts on various supports.[24] To date, the most effective catalysts for the liberation of hydrogen from AB include Pt and Rh on various different types of supports, such as carbon or silica.[51]

Though these are the best catalysts for this reaction, noble metals such as Pt and Rh are rare and expensive. In order to make this technology sustainable and widely used, catalysts must be discovered that are composed of cheap, Earth abundant elements. Additional insights into the mechanism of the catalytic hydrolysis of ammonia borane would be helpful in determining the ways to design and discover catalysts that would be earth-abundant.

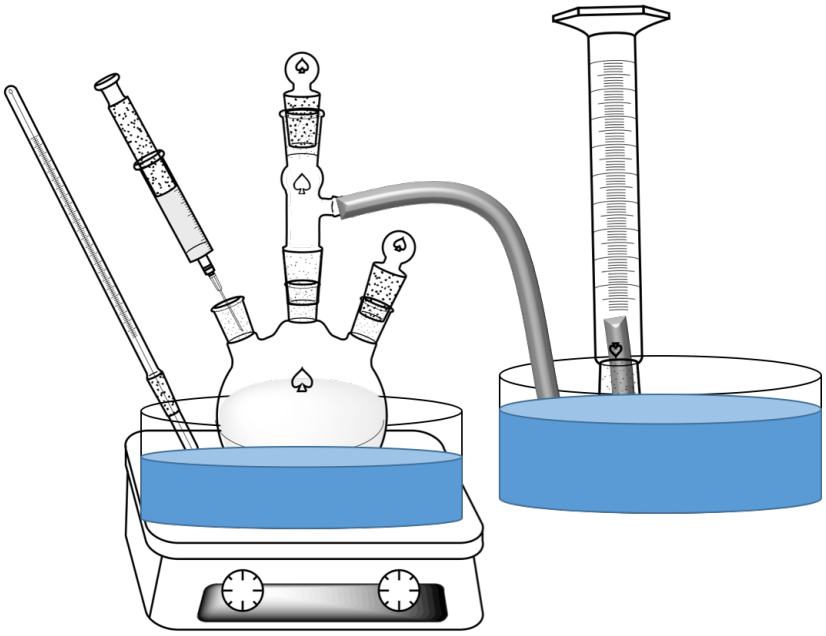

Figure 9: An example of a reaction setup to determine amount of hydrogen gas produced as described by Jiang and Xu.[22]

Chapter 3.2 Experimental

Materials and chemicals:

The following materials were used as purchased without further purification: ruthenium chloride hydrate [98%, $RuCl_3 \bullet H_2O$, Sigma Aldrich], calcium chloride dihydrate [98%, $CaCl_2 \bullet 2H_2O$,

EMD Millipore], barium chloride dihydrate [99%, $BaCl_2 \bullet 2H_2O$, Alfa-Aesar], strontium chloride hexahydrate [99%, $SrCl_2 \bullet 6H_2O$, Alfa-Aesar], potassium hydroxide [100%, KOH, EMD Millipore], ammonia borane [97%, NH3-BH3, Sigma Aldrich].

Synthesis of ruthenates for catalysis:

The coprecipitation synthesis of these catalysts was adapted from previous works.[52] Stoichiometric amounts (1:1 molar ratios) of $RuCl_3 \bullet H_2O$ and $SrCl_2 \bullet 2H_2O$, $CaCl_2 \bullet 2H_2O$, or $BaCl_2 \bullet 2\ H_2O$ were dissolved in ultrapure water and stirred using magnetic stirbar for 5 minutes. 3 M KOH solution was added with stirring until the pH was above 13. After stirring for 1 hour, the solution was allowed to stand for 3 hours and was then washed with water via centrifugation to remove excess salts. The precipitate was dried in an oven at 70˚C overnight in order to remove excess water. The resulting black powder was ground using a mortar and pestle for 10 minutes. The powder was then placed in a box furnace for 5 hours at 600˚C, 800˚C, or 900˚C for $SrRuO_3$, $CaRuO_3$, or $BaRuO_3$, respectively.

Synthesis of RuO_2:

RuO_2 was synthesized via annealing $Ru(III)Cl_3 \bullet H_2O$ in air at 1000˚C for 24 hours.

Synthesis of bulk powders:

Bulk powders were synthesized by grinding their precursors (Table 1) together in a mortar and pestle for 10 minutes. The powders were then pressed into a pellet and fired in a furnace at

1100˚C for 24 hours under ambient conditions. The powders were characterized by X-ray diffraction.

Table 1: Precursors used to synthesize bulk powders

Material	Precursors
$SrRuO_3$	$RuO_2 + SrCO_3$
$CaRuO_3$	$RuO_2 + CaCO_3$
$BaRuO_3$	$RuO_2 + BaCO_3$
$CaMnO_3$	$CaCO_3 + MnO_2$
$LaNiO_3$	$NiO + La_2O_3$
Sr_4IrO_x + $Sr_5Ir_3O_x$	$IrO_2 + SrCO_3$
$SrIrO_3$	$IrO_2 + SrCO_3$
$BaMnO_3$	$BaCO_3 + MnO_2$
Ca_2IrO_4	$IrO_2 + CaCO_3$
$SrSmO_3$	$SrCO_3 + Sm_2O_3$
$MnTiO_3$	$MnO_2 + TiO_2$
$SrFeO_3$	$Fe_2O_3 + SrCO_3$
$BaMnO_3$	$BaCO_3 + MnO_2$
$Ba_3SrRu_2O_x$	$RuO_2 + BaCO_3 + SrCO_3$

Catalytic testing:

A flask, equipped with the catalyst and a stirbar, was contained via rupper septum. A needle and plastic tubing connected the closed flask to an inverted graduated cylinder full of water and submerged in a crystallization dish. Ammonia borane (30.8 mg, 1 mmol) was dissolved in 2.6 mL of water and injected into the flask containing the catalyst. The quantity of hydrogen produced was measured using the amount of water displaced using the graduated cylinder.

Materials characterization:

Powder X-ray diffraction (XRD) patterns were acquired using a Bruker-AXS D8 Advance diffractometer with CuKα radiation and a LynxEye 1-D detector. Simulated XRD patterns were generated using the Crystal-Maker/CrystalDiffract software package.

Chapter 3.3 Results & Discussion

A screening process for catalysts took place by testing bulk metal oxide powders in order to see whether they were effective catalysts for the hydrolysis of AB. $LaFeO_3$, $SrFe_2O_5$, and $Sr_3Fe_2O_9$ were each inactive, as no hydrogen was liberated. However, this screening method revealed that bulk strontium ruthenate in the 1:1 phase ($SrRuO_3$) produced the full yield of 3 molar equivalents of hydrogen in less than an hour (Fig 10).

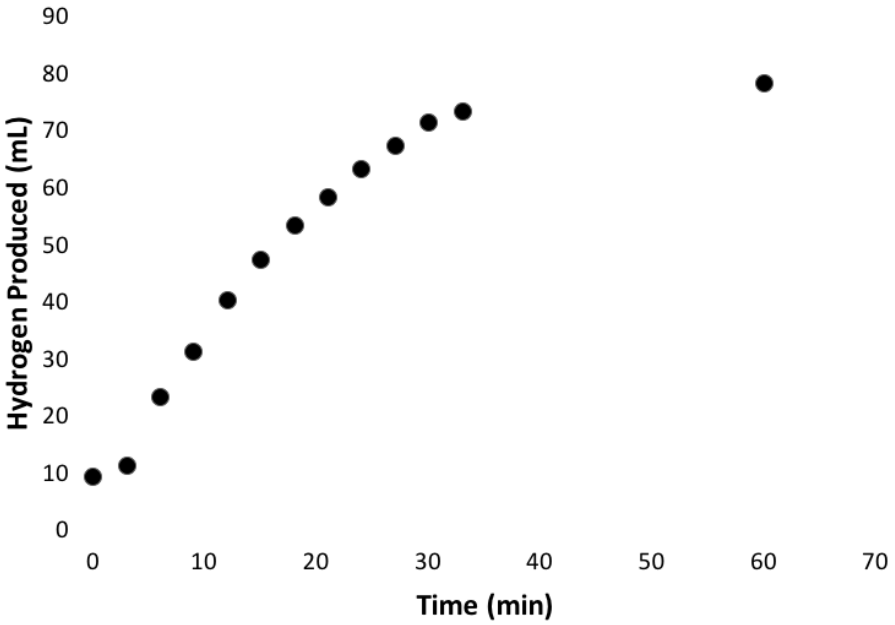

Figure 10: Bulk SrRuO3 catalyzed the AB hydrolysis and resulted in 3 molar equivalents being produced in less than 1 hour.

Due to the catalytic activity of $SrRuO_3$, similar systems were tested. RuO_2 was tested from the shelf as purchased and synthesized via annealing at high temperatures. Both of these systems were found to be less active (Fig. 11). The synthesized RuO_2 achieved 75% yield of hydrogen after 2.5 hours, while the purchased RuO_2 was produced no hydrogen over 2.5 hours.

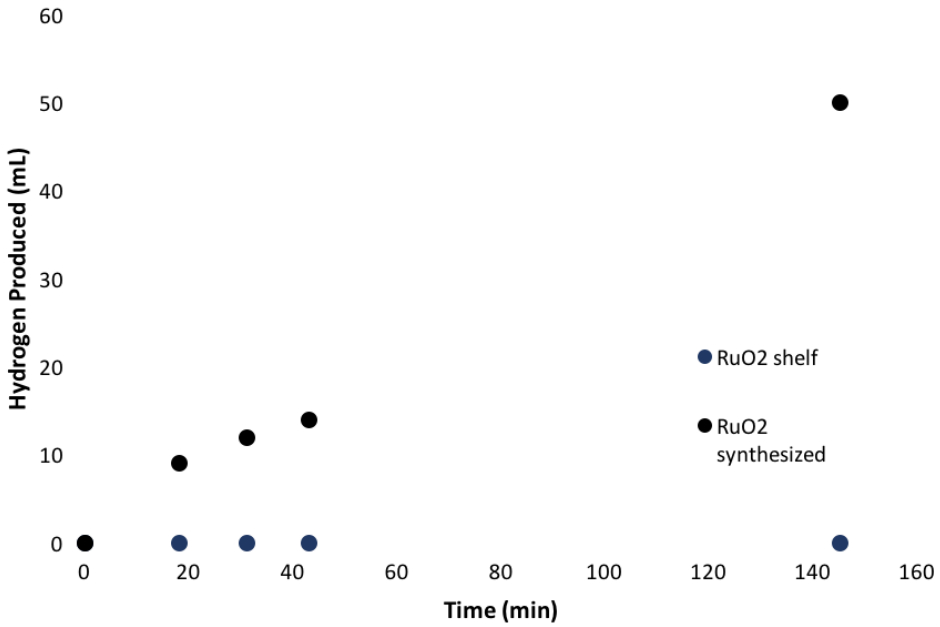

Figure 11: Catalytic activity of synthesized and purchased RuO_2.

Additionally, other systems were tested due to their similarities to the active $SrRuO_3$ catalyst. SrO was tested due to the alkaline earth metal, but no catalytic activity observed after 30 minutes. Calcium and barium ruthenate in the 1:1 phases were also tested in order to determine whether the effect of the alkaline earth metal on the catalytic activity. These two materials were active for catalysis, achieving a rate of ~ 1 mL hydrogen/minute, and were therefore of interest to be studied further (Fig. 12). Additionally, $CaMnO_3$, $BaMnO_3$, $SrFeO_3$, $MnTiO_3$, $SrSmO_3$, Ca_2IrO_4, $BaMnO_3$, $SrIrO_3$, $Sr_4IrO_x + Sr_5Ir_3O_x$, $Ba_3SrRu_2O_x$, $LaNiO_3$ were each tested and were found to be inactive catalysts, producing little to no hydrogen after a testing period of 30 minutes.

Table 2: Screening of catalysts which did not produce more than 3 mL of hydrogen after 30 minutes.

Material	Hydrogen Produced in 30 min (mL)
$CaMnO_3$	1
$LaNiO_3$	0.5
$Sr_4IrO_x + Sr_5Ir_3O_x$	2
$SrIrO_3$	2
$BaMnO_3$	2
Ca_2IrO_4	2
$SrSmO_3$	0.5
$MnTiO_3$	1
$SrFeO_3$	2
$BaMnO_3$	0
$Ba_3SrRu_2O_x$	3

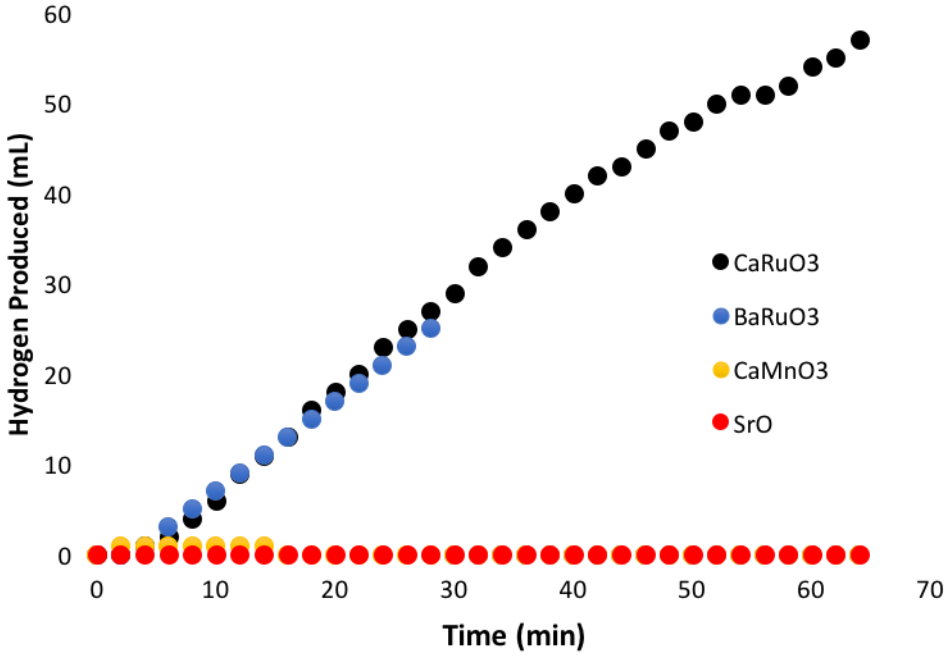

Figure 12: Other catalysts with similar chemical properties were tested for AB hydrolysis. $BaRuO_3$ and $CaRuO_3$ were each effective.

Several methods were explored in order to synthesize the bulk ruthenates on the nanoscale to achieve higher surface area and therefore more active catalysts. Coprecipitation methods published previously were used to synthesize nanoscale calcium, barium, and strontium ruthenates in 1:1 stoichiometry.[52] Here, these nanoscale catalysts were produced with slight ruthenium oxide impurities , as confirmed via XRD (Figs 13-15).

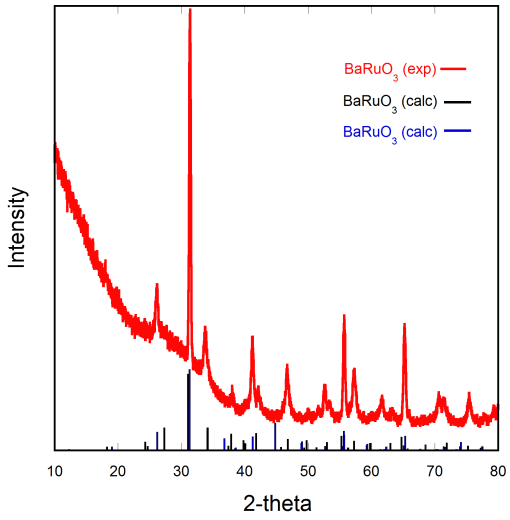

Figure 13: X-ray diffraction pattern confirming the synthesis of $BaRuO_3$.

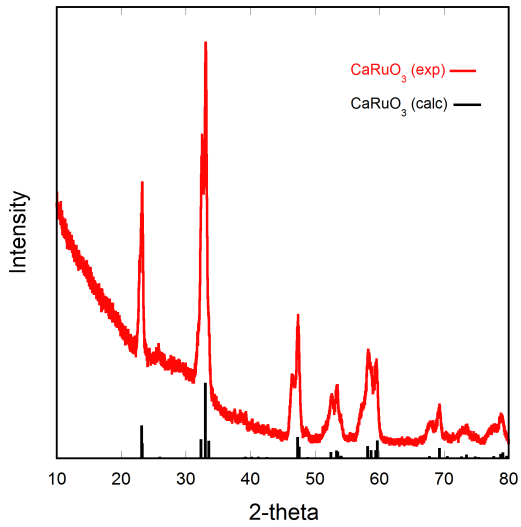

Figure 14: X-ray diffraction pattern confirming the synthesis of $CaRuO_3$.

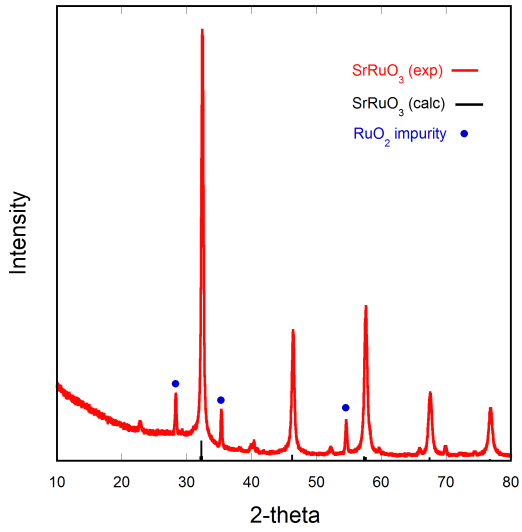

Figure 15: X-ray diffraction confirmed the synthesis of $SrRuO_3$. Small impurities of RuO_2 were present as well.

These ruthenate catalysts, when synthesized using these methods, produced hydrogen at a higher rate by the hydrolysis of AB (Fig. 16, Table 2).

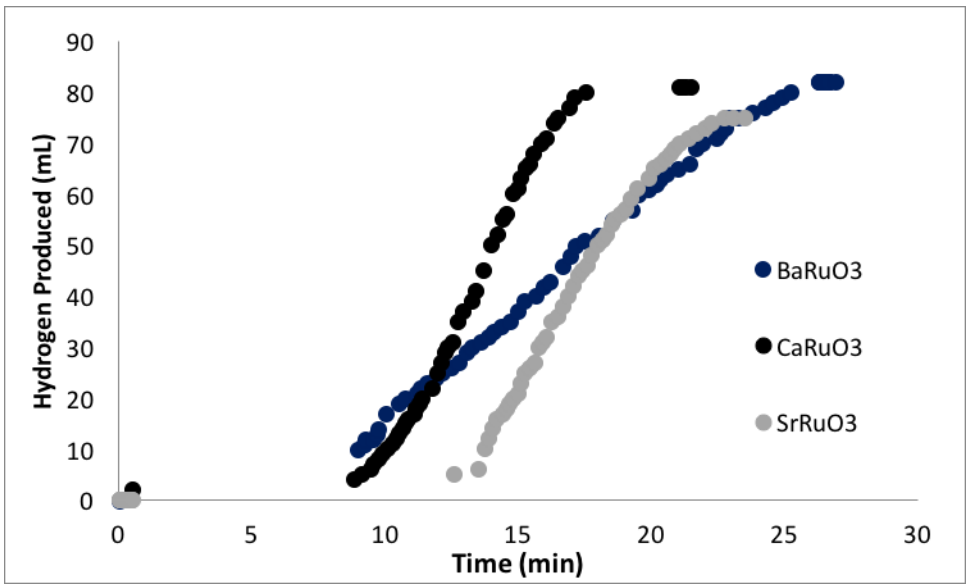

Figure 16: Nanoscale $SrRuO_3$, $CaRuO_3$, and $BaRuO_3$ were active catalysts for AB hydrolysis.

Table 3: Rates of hydrogen production using ruthenate catalysts, calculated using the active time period of the reaction (from when the reaction began producing hydrogen to when it reached the full yield).

Material	Overall Rate (mL min^{-1})	Time to Reach Full H_2 Yield (min)
$CaRuO_3$	8.44	16.95
$SrRuO_3$	6.90	21.38
$BaRuO_3$	4.32	25.25

Reaching the full yield of hydrogen within 20 minutes is comparable to some of the reported catalysts for this reaction.[51,53,54] Though they do take longer than some of the reported catalysts, there are no reliable reports of oxides being used to catalyze this reaction. Additionally, the surface area of this material is not accounted for, and will be used to calculate the turnover value. This turnover value will be compared to the published catalysts for this reaction.

This use of ruthenates for the hydrolysis of AB is the first reliable use of oxides to catalyze this reaction. Additionally, some mechanistic details of the catalytic hydrolysis may be obtained by the knowledge that RuO_2 is an ineffective catalyst for this reaction, but the Ru (IV) oxidation state is facilitating the hydrolysis in the perovskite form.

Chapter 3.4 Conclusions

In this work, calcium, strontium, and barium ruthenates in the 1:1 stoichiometry were successfully used to catalyze the hydrolysis of ammonia borane to produce 3 molar equivalents of hydrogen. This is the first reliable reporting of oxides catalyzing this reaction and releasing the full molar yield of AB. The use of these specific ruthenates may be useful in understanding the mechanistic details of the catalytic hydrolysis of AB, as ruthenium oxide is an ineffective catalyst for this reaction.

Chapter 3.5 Future Work

There is certainly more work to be done to discover the full potential of ruthenates for the catalysis of AB. The material must be characterized in order to determine its surface area and the turnover frequency should be calculated after normalizing for surface area. DFT calculations may be an effective way to learn about the mechanistic details of this reaction, comparing the activities of Ru^0 metal with RuO_2 and $ARuO_3$ (A=Ca,Sr,Ba).

References

(1) Lewis, N. S.; Nocera, D. G. *Proc. Natl. Acad. Sci. U. S. A.* **2003**, *100* (24), 14187–14192.

(2) Dresselhaus, M.; Thomas, I. *Nature* **2001**, *414* (November).

(3) Read, C. G.; Callejas, J. F.; Schaak, R. E.; Lewis, N. S.; Roske, C. W. **2016**.

(4) Staff, EIA. Monthly Energy Review.

(5) Climate Change Indicators: Atmospheric Concentrations of Greenhouse Gases.

(6) Lewis, N. S. *MRS Bull.* **2007**, *32* (10), 808–820.

(7) Peters, G. P.; Andrew, R. M.; Boden, T.; Canadell, J. G.; Ciais, P.; Quéré, C. Le; Marland, G.; Raupach, M. R.; Wilson, C. *Nat. Clim. Chang.* **2013**, *3* (January), 4–6.

(8) Smith, P.; Davis, S. J.; Creutzig, F.; Fuss, S.; Minx, J.; Gabrielle, B.; Kato, E.; Jackson, R. B.; Cowie, A.; Kriegler, E.; van Vuuren, D. P.; Rogelj, J.; Ciais, P.; Milne, J.; Canadell, J. G.; McCollum, D.; Peters, G.; Andrew, R.; Krey, V.; Shrestha, G.; Friedlingstein, P.; Gasser, T.; Grubler, A.; Heidug, W. K.; Jonas, M.; Jones, C. D.; Kraxner, F.; Littleton, E.; Lowe, J.; Moreira, J. R.; Nakicenovic, N.; Obersteiner, M.; Patwardhan, A.; Rogner, M.; Rubin, E.; Sharifi, A.; Torvanger, A.; Yamagata, Y.; Edmonds, J.; Yongsung, C. *Nat. Clim. Chang.* **2016**, *6* (1), 42–50.

(9) Zou, X.; Zhang, Y. *Chem. Soc. Rev.* **2015**, *44*, 5148–5180.

(10) Balema, V. *Hydrogen Storage Materials*; 2007; Vol. 2.

(11) IEA. **2015**, 81.

(12) Srinivasan, S.; Mosdale, R.; Stevens, P.; Yang, C. *Annu. Rev. Energy Environ.* **1999**, *24* (1), 281–328.

(13) Fukuzumi, S.; Yamada, Y.; Suenobu, T.; Ohkubo, K.; Kotani, H. *Energy Environ. Sci.* **2011**, *4* (8), 2754.

(14) Office of Energy Efficiency and Renewable. Hydrogen Production: Natural Gas Reforming | Department of Energy http://energy.gov/eere/fuelcells/hydrogen-production-natural-gas-reforming.

(15) Kudo, A.; Miseki, Y. *Chem. Soc. Rev.* **2009**, *38* (1), 253–278.

(16) Steele, B. C.; Heinzel, A. *Nature* **2001**, *414* (6861), 345–352.

(17) Huang, C.; T-Raissi, A. *J. Power Sources* **2008**, *175* (1), 464–472.

(18) Miller, E. *Energy Environ. Sci.* **2007**, *61* (10), 815–819.

(19) Read, C.; Thomas, G.; Ordaz, G.; Satyapal, S. *Matrial Matters* **2007**, *2* (2), 3–4.

(20) A. Karkamkar T. Autrey, C. A. **2007**, *2* (2), 6–9.

(21) Sun, D.; Mazumder, V.; Metin, Ö.; Sun, S. *ACS Catal.* **2012**, *2* (6), 1290–1295.

(22) Jiang, H. L.; Xu, Q. *Catal. Today* **2011**, *170* (1), 56–63.

(23) McEnaney, J. M.; Chance Crompton, J.; Callejas, J. F.; Popczun, E. J.; Biacchi, A. J.; Lewis, N. S.; Schaak, R. E. *Chem. Mater.* **2014**, *26* (16), 4826–4831.

(24) Chandra, M.; Xu, Q. *J. Power Sources* **2007**, *168* (1 SPEC. ISS.), 135–142.

(25) McEnaney, J. M.; Soucy, T. L.; Hodges, J. M.; Callejas, J. F.; Mondschein, J. S.; Schaak, R. E. *J. Mater. Chem. A* **2016**, *4* (8), 3077–3081.

(26) Walter, M. G.; Warren, E. L.; McKone, J. R.; Boettcher, S. W.; Mi, Q.; Santori, E. A.; Lewis, N. S. *Chem. Rev. (Washington, DC, United States)* **2010**, *110* (11), 6446–6473.

(27) Gray, H. B. *Nat. Chem.* **2009**, *1* (1), 7.

(28) Vesborg, P. C. K.; Seger, B.; Chorkendorff, I. *J. Phys. Chem. Lett.* **2015**, *6* (6), 951–957.

(29) Popczun, E. J.; McKone, J. R.; Read, C. G.; Biacchi, A. J.; Wiltrout, A. M.; Lewis, N. S.; Schaak, R. E. *J. Am. Chem. Soc.* **2013**, *135* (25), 9267–9270.

(30) McCrory, C. C. L.; Jung, S.; Ferrer, I. M.; Chatman, S. M.; Peters, J. C.; Jaramillo, T. F. *J. Am. Chem. Soc.* **2015**, *137* (13), 4347–4357.

(31) Jin, J.; Walczak, K.; Singh, M. R.; Karp, C.; Lewis, N. S.; Xiang, C. *Energy Environ. Sci. Energy Environ. Sci* **2014**, *7* (7), 3371–3371.

(32) Hinnemann, B.; Moses, P. G.; Bonde, J.; Jorgensen, K. P.; Nielsen, J. H.; Horch, S.; Chorkendorff, I.; Nørskov, J. K. *J. Am. Chem. Soc.* **2005**, *127* (15), 5308–5309.

(33) Vrubel, H.; Hu, X. *Angew. Chemie - Int. Ed.* **2012**, *51* (51), 12703–12706.

(34) Mcenaney, J. M.; Crompton, J. C.; Callejas, J. F.; Popczun, E. J.; Biacchi, A. J.; Lewis, N. S.; Schaak, R. E. **2014**.

(35) McKone, J. R.; Sadtler, B. F.; Werlang, C. A.; Lewis, N. S.; Gray, H. B. *ACS Catal.* **2013**, *3* (2), 166–169.

(36) Kublanovsk, V. S.; Yapontseva, Y. S. *Electrocatalysis* **2014**, *5*, 372.

(37) Baeck, S. H.; Choi, K. S.; Jaramillo, T. F.; Stucky, G. D.; McFarland, E. W. *Adv. Mater.* **2003**, *15* (15), 1269–1273.

(38) Popczun, E. J.; Read, C. G.; Roske, C. W.; Lewis, N. S.; Schaak, R. E. *Angew. Chemie - Int. Ed.* **2014**, *53* (21), 5427–5430.

(39) Soloveichik, G. L. *Mater. Matters* **2007**, *2* (2), 11–14.

(40) Targets for on-board hydrogen storage systems : Current R & D focus is on 2010 Targets http://www1.eere.energy.gov/hydrogenandfuelcells/pdfs/freedomcar_targets_explanations.pdf.

(41) Shore, S. G.; Parry, R. W. *J. Am. Chem. Soc.* **1958**, *80* (1), 8–12.

(42) Sanyal, U.; Demirci, U. B.; Jagirdar, B. R.; Miele, P. *ChemSusChem* **2011**, *4*, 1731–1739.

(43) Zhu, Q.-L.; Xu, Q. *Energy Environ. Sci.* **2015**, *8* (2), 478–512.

(44) Chandra, M.; Xu, Q. *J. Power Sources* **2006**, *156* (2), 190–194.

(45) Xu, Q.; Chandra, M. *J. Alloys Compd.* **2007**, *446–447*, 729–732.

(46) Himmelberger, D. W. Hydrogen Release From Ammonia Borane, 2010.

(47) Bluhm, M. E.; Bradley, M. G.; Iii, R. B.; Kusari, U.; Sneddon, L. G. **2006**, *3*, 7748–7749.

(48) Himmelberger, D. W.; Alden, L. R.; Bluhm, M. E.; Sneddon, L. G. *Inorg. Chem.* **2009**, *48* (20), 9883–9889.

(49) Yan, J.; Zhang, X.; Han, S.; Shioyama, H.; Xu, Q. *Angew. Chemie Int. Ed.* **2008**, 2287–2289.

(50) Metin, Ö.¨; Mazumder, V.; Özkar, S.; Sun, S. *J. Am. Chem. Soc.* **2010**, *132* (5), 1468–1469.

(51) Zhan, W.; Zhu, Q.-L.; Xu, Q. *ACS Catal.* **2016**, acscatal.6b02209.

(52) Atta, N. F.; Galal, A.; Ali, S. M. *Int. J. Electrochem. Sci.* **2012**, *7*, 725–746.

(53) Peng, C.-Y.; Kang, L.; Cao, S.; Chen, Y.; Lin, Z.-S.; Fu, W.-F. *Angew. Chemie Int. Ed.* **2015**.

(54) Yang, X.; Hall, M. B. *J. Am. Chem. Soc.* **2008**, *130* (6), 1798–1799.

Academic Vita

Taylor L. Soucy

Education

The Pennsylvania State University, University Park, PA
Spring 2017
Schreyer Honors College, Millennium Scholars Program
Bachelors of Science in Chemistry, American Chemical Society Certified

Research Experience

The Pennsylvania State University, University Park, PA
Dr. Raymond Schaak
Undergraduate Researcher (May 2014-Present)
Synthesized electrocatalytic nanoparticles for the formation and release of hydrogen and for the evolution of oxygen, and characterized materials using transmission electron microscopy and X-ray diffraction

Unilever Corp. Trumbull, CT
Research & Development Intern (June-August 2016)
Developed new products for Dove Premium brand, and modeled prototype as a function of formulation

University of California, Santa Barbara. Santa Barbara, CA
National Nanotechnology Infrastructure Network (NNIN) REU
Dr. Mark D'Evelyn, Soraa Inc.
Undergraduate Researcher (June-August 2016)
Performed cleanroom techniques to map stress due to sputter deposition & gold electroplating when synthesizing thin films

Publications

(2) McEnaney, J.M; **Soucy, T.L**; Hodges, J.M; Callejas, J.F; Mondschein, J.S; Schaak, R.E. Colloidally-synthesized cobalt molybdenum nanoparticles as active and stable electrocatalysts for the hydrogen evolution reaction under alkaline conditions. *Journal of Materials Chemistry A*. **2016** *4*, 3077-3081.

(1) **Soucy, T.L** "Measurement and Management of Thin Film Stresses"; 2015 NNIN REU Research Accomplishments, 182-183, http://nnin.org/reu/past-years/2015-nnin-reu-program, November 2015.

Presentations

(6) Soucy, T.L; Mondschein, J. S; McEnaney, J. M; Badding, C.K; Schaak, R.E. The Discovery of Earth Abundant Catalysts Towards the Implementation of a Hydrogen Economy. The National American Chemical Society Meeting. San Francisco. April 2-4 2017. Abstract Submitted.

(5) Soucy, T.L; Jiang, K; Cook, J; Tran, A; D'Evelyn, M. Measurement and Management of Thin Film Stresses. Local American Chemical Society Meeting. The Pennsylvania State University, University Park, PA; September 8, 2015. Contributed Poster.

(4) Soucy, T.L; Jiang, K; Cook, J; Tran, A; D'Evelyn, M. Measurement and Management of Thin Film Stresses. National Nanotechnology Infrastructure Network REU Convocation. Cornell University, Ithaca, NY. August 8-13, 2015. Contributed Talk & Poster.

(3) Soucy, T. L; Popczun, E; Schaak, R. E. Metal Ferrite Nanoparticles as Catalysts for the Oxygen Evolution Reaction. Howard Hughes Medical Institute Scholars Retreat Conference. October 4, 2014. Winterfell, Virginia. Contributed Poster.

(2) Soucy, T. L; Popczun, E; Schaak, R. E. Metal Ferrite Nanoparticles as Catalysts for the Oxygen Evolution Reaction. Eberly College of Science Undergraduate Research Symposium. Penn State University, University Park, PA, September 25, 2014. Contributed Poster.

(1) Soucy, T. L; Popczun, E; Schaak, R. E. Metal Ferrite Nanoparticles as Catalysts for the Oxygen Evolution Reaction**.** July 31, 2014. 2014 Penn State Research Symposium. Contributed Poster, Contributed Talk.

Work Experience

The Pennsylvania State University, University Park, PA
Dr. Raymond Funk
Teaching Assistant, Organic Chemistry II (January 2016-May 2016)

- Taught students during homework review sessions
- Graded exams and homework assignments
- Assisted students during office hours

The Pennsylvania State University, University Park, PA
Starlette Sharp, Millennium Scholars Program
Tutor, Organic Chemistry I & Organic Chemistry II (September 2015-Present)

- Assisted students in studying for exams & completing homework assignments

Awards & Honors

- Penn State Dean's List (2013-2016)
- Homer F. Braddock College of Science Memorial Scholarship (2013-2016)
- Lewis A. and Opal D. Gugliemelli Honors Scholarship in Science (2016)
- K. Elizabeth Howe Memorial Scholarship (2016)
- Dalton Undergraduate Student Research Fund for Women in the Sciences (2016)
- Baynard and Ethel Kunkle Scholarship (2016)
- Herbert H. and Beatrice S. Meyer Alumni Memorial Scholarship (2013-2016)
- Lauren E. and Samuel B. Bonsall Trustee Scholarship for Schreyer Honors College (2015-2016)
- Army Emergency Relief MG James Ursano Scholarship (2016, 2014)
- Folds of Honor Scholarship (2013-2016)
- Marion J. Eyster Scholarship (2015)
- Norman Freed Undergraduate Research Award in Eberly College of Science (2015)

- Meredith M. Gee Scholarship in Science (2014)
- Delaware Scholarship Incentive Program (2013, 2014)
- Millennium Scholar (2013-present)
- Schreyer Honors College Scholar (2013-present)

Memberships/Service

The American Chemical Society
Student Member (2015-Present)

Undergraduate Research Society, Penn State, University Park, PA
Member; Mentor; Physical Sciences Liaison (August 2015-Present)

- Mentored underclassmen when choosing research labs
- Communicated with College of Science faculty
- Expanded lab tours into physical sciences department

Millennium Scholars Program, Penn State, University Park, PA
Council Member; Member (August 2013-Present)

- Engaged women of the program
- Generated mentorship within the program
- Mentored group of students throughout the year